Control of average size and size distribution in as-grown nanoparticle polymer composites of MSe (M = Cd or Zn)

Stephen W. Haggata,[a] David J. Cole-Hamilton*[a] and John R. Fryer[b]

[a]*School of Chemistry, University of St. Andrews, St. Andrews, Fife, Scotland, UK KY16 9ST*

[b]*Department of Chemistry, Glasgow University, Glasgow, Scotland, UK G12 8QQ*

The preparation of CdSe and ZnSe semiconductor nanoparticles in the quantum size regime (1–5 nm) within a polymer matrix is described. A carefully controlled reaction temperature and suitable choice of solvent is found to have a dramatic effect on the size of the particles produced when a soluble pyridyl polymer adduct (a polymer that contains nitrogen and dimethylcadmium or dimethylzinc) is reacted with H_2Se in solution. An expected change in colour (absorbance) of the material from black through to yellow is observed for cadmium selenide and dark yellow to light yellow for zinc selenide as the particles decrease in size. TEMs reveal that cadmium selenide particles are evenly distributed in the polymer film with a size distribution wider than analogous sulfide preparations recently reported. The CdSe particles exhibit size quantization and hence a blue shift of the band edge position is observed in the absorbance and photoacoustic spectra as the reaction temperature is decreased or the polymer solubility is improved. ZnSe nanoparticle growth has been found difficult to control although a change in reaction temperature has an effect on the particle size similar to that for CdSe.

Semiconductor nanosized particles (or QDs) are small molecular clusters in the size range of *ca.* ten to several hundred ångströms in diameter and have attracted considerable research interest during the last several years because of their unique quantum effects observed only at nanosized dimensions and which lead to obvious differences from bulk macrocrystallites in terms of their electronic, optical and catalytic properties.[1–16] These materials have possible future applications as photocatalysts in photoreactions,[4,13] in electro-luminescent devices (electro-optics)[8,9,10] for *e.g.* the development of flat panel luminescent displays; photoconductive and photovoltaic devices[11,12] in *e.g.* photocopiers and laser printers; all-optical (non-linear optical)[14] devices in *e.g.* optical switches; and magneto-optics[15] in *e.g.* erasable optical data storage. However, there are important criteria that have to be met before such devices can be realised. The first is the preparation of a high concentration of monodisperse particles. The size and shape of the particles has an influence on the wavelength of their absorbance and light emission which can be 'tuned' by altering the particle size. Therefore, narrow size distributions are essential if pure colours are to be obtained in luminescence. A second, vital point is the control of the surface (grain boundary). A substantial percentage of crystallite atoms are surface atoms and these largely account for the chemical and physical properties of the particle. Therefore, in order to prevent higher wavelength emission, surface states must be eradicated and this can be achieved by chemically binding the particles to a suitable material of higher band gap.[4,5] Polymers are able to passivate the material and prevent particle agglomeration whilst maintaining a good spatial distribution of particles. In some cases polymers are able to assist charge transfer in *e.g.* photoconductive and electroluminescent devices. Here, it is essential to encapsulate the crystallites in a conducting polymer in order for charge extraction to proceed.[11,12] There are many synthetic methods reported which target surface control and monodispersity and these include syntheses in colloidal suspensions,[17,18] solutions of single-molecule precursors,[19,20] sol–gels,[21] zeolites,[22] LB films,[23] micelles[7,24] and polymer films.[8–11] Of these methods, the formation of semiconductor nanosized particles in a polymer medium has received intense interest owing to the ready processibility of the polymer films and possible future application in device structures.[8–11,25–31] The synthesis of nanosized semiconductor particles in a polymer matrix in the past has usually involved the passing of a chalcogenide gas over the surface of a polymer blend or co-polymer film which contains either organometallic blocks[32,33a,b] which have a complex synthesis, or coordinated metal salts.[34] The microphase separation domains in the block copolymer are able to control the particle dispersity and size distribution. However, these methods are carried out in a heterogeneous phase and consequently very low loading of semiconductor particles and varying metal/chalcogenide stoichiometry is observed if the morphology of the polymer film is poorly controlled. An alternative approach is to mix preprepared particles with suitable polymers and then use the composite to form films.[8,9,11,35] Methods in which the particle film composite is formed '*in situ*' by using a soluble polymer/metal complex adduct and reacting it with a suitable source of the group 16 element have been less explored, but is the basis for the successful production of nanoparticulates from aqueous solutions containing polyphosphates.[36] In these systems, the polymer not only acts as the encapsulant for the particles, but is also capable of controlling the particle size by providing slow release of group 12 precursor and by binding to surface metal atoms to terminate the particle growth. Recently,[10] the copolymerisation of styrene and zinc methacrylate to form a soluble zinc containing microgel and subsequent reaction with H_2S has produced ZnS nanocrystals in a polymer matrix. How luminescent devices can be made from such composite materials has also been described.[10]

Our previous work has described the functionalization of polybutadiene with various Lewis-base groups by homogeneous catalysis[37–39] to form soluble polymer ligands. Further, we have reported that the addition of group 12 metal alkyls forms soluble metal alkyl/polymeric adducts[40] and we have then observed their reaction with hydrogen sulfide gas[41,42] to form semiconductor colloids. Polymer/semiconductor composite films can then be obtained after removing the solvent under vacuum or by filtration which has proved a simple, flexible and alternative route to the preparation of nanoparticulate II/VI materials with narrow size dispersion. Particular advantages of this technique include the low reaction temperatures involved, the simplicity of the system, and especially the ability to obtain polymer nanoparticle composites in which the particle size distribution is narrow without subsequent treatment or size fractionation. The average particle

size can be controlled over a wide range by controlling the reaction parameters, especially temperature. The polymer/metal alkyl adducts readily dissociate on heating,[43] so they may also be useful for purifying metal alkyls through the adduct purification process[44] although simpler systems based on monomeric Lewis bases are currently preferred because of their lower cost.

Experimental

Experiments were carried out under dry oxygen-free argon purified by passing through a series of columns consisting of Cr^{2+} on silica and dry molecular sieves. Greaseless joints and taps were employed and manipulations were carried out using standard Schlenk-line and catheter tubing techniques. All the solvents were carefully dried by distillation from sodium diphenylketyl. 2-Methylpyridine was purchased from Aldrich and was distilled prior to use. Butyllithium (1.6 M in hexane) and dimethylzinc (2.0 mol dm^{-3} in toluene) were purchased from Aldrich and used as received. Polybutadiene (83% pendant, 17% *trans*-1,4, $M_n = 3000$) was a commercial product (Nippon Soda Company) and was used after pumping for 2 h. Me_2Cd was prepared by the standard literature method.[45]

Powder X-ray diffraction (PXRD) patterns were recorded on a Stöe STADI/P diffractometer using Cu-Kα radiation. Data were collected in transmission mode with a sample mounted in vaseline on a rotating disc and compared with the standard pattern obtained from the JCPDS database or the PXRD pattern of a wurtzite sample.

Transmission electron micrographs (TEMs) were obtained using a Phillips EM 301 microscope at 80 keV. All samples were embedded in an epoxy resin and the sections were then cut on a microtome with a diamond knife. The dried specimen sections were put onto a copper grid which had a carbon support film present. Another layer of carbon was then evaporated onto the sample in order to prevent specimen charging. High resolution TEMs (HRTEMs) were obtained by using an ABT 002B microscope at 200 keV. The samples were either prepared as previously described or suspended in acetone and then ultrasonically dispersed and lifted off onto a graphite grid.

Both absorbance and photoacoustic spectroscopy (PAS) were used to measure the band edge of the material. Photoacoustic spectra were obtained using an OAS 400 photoacoustic spectrophotometer as described previously.[42] Absorbance spectra were obtained using a Perkin Elmer Lambda 14P UV–VIS spectrophotometer. All samples were scanned from the UV region to the near IR (300–800 nm). The knees of the band edge for both photoacoustic and absorption spectra were recorded and taken as the closest estimation of the band edge value. Of course, the particle size distribution of the material will directly affect the slope of the band edge and therefore calculated band gap values are indicative of the smallest sized particles only. For commercial CdSe (cadmoselite), the value of the band edge measured in this way is 1.74 eV (lit. value, 1.74 eV[46]). Calculations of the band gap when the band edge value is taken from the tail of the spectrum are more inaccurate as the band edge is smeared out by lattice vibrations and falls off exponentially in accordance with Urbach's rule.[47,48]

Synthesis of a polymer adduct with dimethylcadmium or dimethylzinc

The polymeric polybutadiene Lewis base containing 2-methylpyridyl (2pySiPB) groups and the subsequent dimethylcadmium or dimethylzinc polymer adduct were synthesized as previously reported.[42] In all cases the M/N (M = Zn, Cd) mole ratio of metal alkyl to coordinating nitrogen was 0.5.

Synthesis of nano-sized CdSe and ZnSe semiconductor particles

The preparation procedure for zinc/polymer composites follows that for cadmium which is now described. A 2pySiPB polymer–dimethyl cadmium solution (3% g cm^{-3} of polymer) stirred in a flask (250 ml) under nitrogen was gradually exposed to a hydrogen selenide atmosphere until a solid precipitated. The transparent yellow polymer adduct solution quickly changed to either a yellow, orange, red, crimson, brown or black coloured suspension of cadmium selenide in polymer (yellow for zinc selenide), the colour depending on the reaction temperature or choice of solvent. As soon as the precipitate was observed, the H_2Se gas flow was interrupted and the suspension was allowed to settle and then separated by filtration isolating the coloured polymer composite.

Results

Reactions in toluene of polypyridine bound Me_2M with H_2Se produce composites consisting of nanoparticles embedded within the polymer matrix (Fig. 1). A series of different coloured CdSe/polymer samples prepared by the method above under various synthesis conditions are illustrated in Fig. 2. The size quantization effect can be seen most dramatically in samples Cd1 [−78 °C, Fig. 2(a)], Cd2 [r.t., Fig. 2(b)] and Cd3 [60 °C, Fig. 2(c)] where a darkening in colour indicates an increase in particle size and a decrease in band gap energy.

The PXRD pattern of Cd3, Fig. 3(c), shows the sharpest and most intense peak in all CdSe patterns at the 2θ value of 25.5° (002), broader *hkl* reflections at 42.0° (110) and 50.0° (112) as well as very broad (103) reflection at 46.0°. These reflections are indicative of the cadmoselite (hexagonal) phase, Fig. 3(e), and not the sphalerite (cubic) phase of CdSe [see the JCPDS pattern of cubic CdSe, Fig. 3(f)]. The hexagonal phase is also confirmed by the lattice spacings in the HRTEM images. The broad peak of the polymer is observed at $2\theta = 17°$.

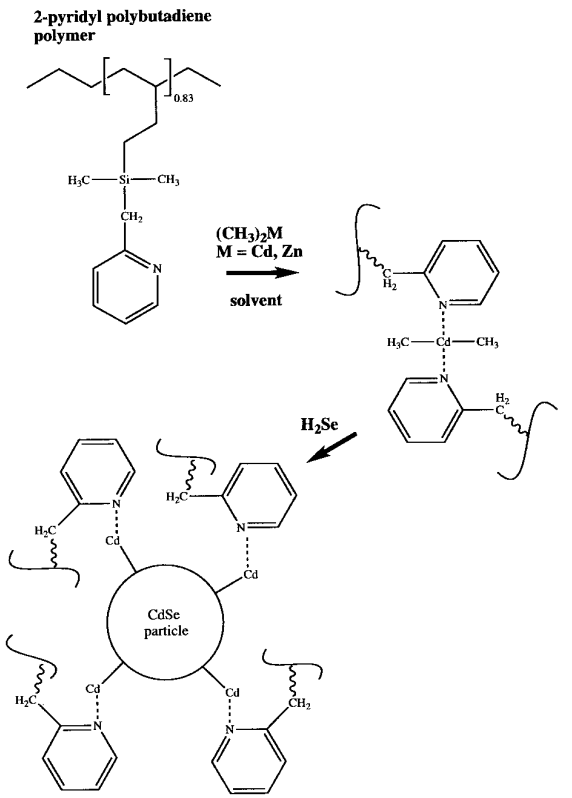

Fig. 1 Formation of the 2pySiPB adduct and the reaction of the polymer adduct with hydrogen selenide

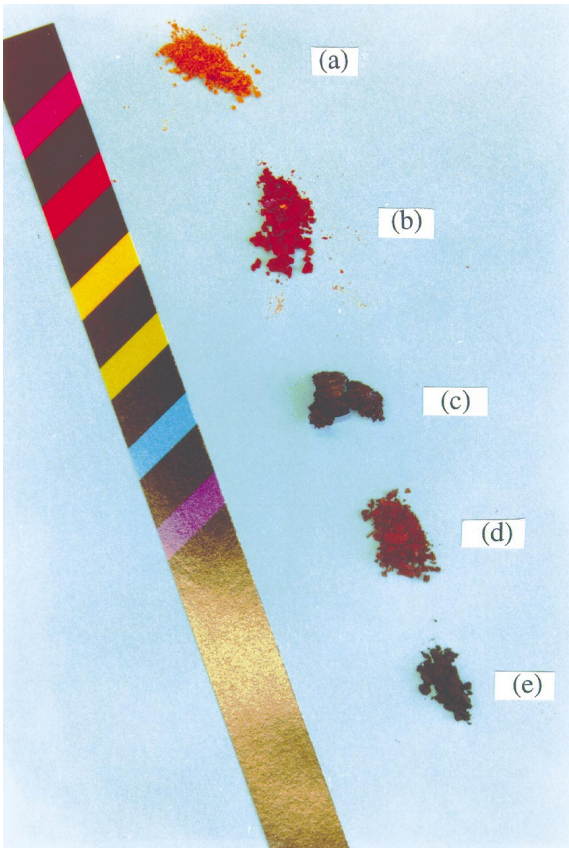

Fig. 2 CdSe samples showing quantum confinement. Samples (a) to (c) were prepared in toluene in the presence of 2pySiPB at (a) −78 °C, run Cd1; (b) 25 °C, run Cd2; and (c) 60 °C, run Cd3. Sample (d) r.t., run Cd4, is prepared in light petroleum in the presence of 2pySiPB. Sample (e) is commercial (bulk) cadmium selenide.

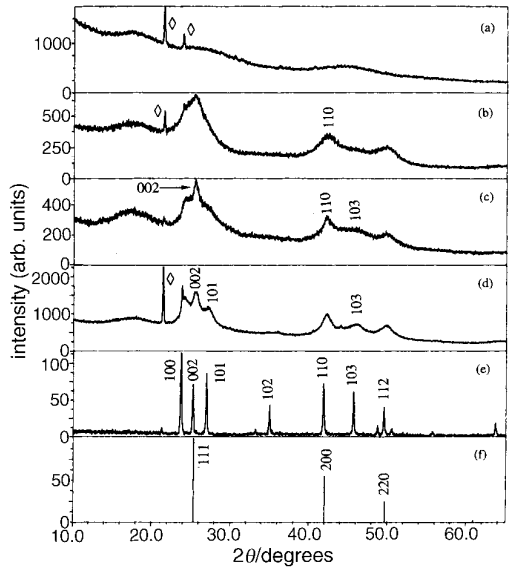

Fig. 3 PXRD patterns of CdSe prepared in toluene in the presence of 2pySiPB at (a) −78 °C, run Cd1; (b) 25 °C, run Cd2; (c) 60 °C, run Cd3. Pattern (d) corresponds to a CdSe sample prepared in petrol in the presence of 2pySiPB, run Cd4. Patterns (e) and (f) correspond to commercial hexagonal (cadmoselite) CdSe and JCPDS pattern for cubic CdSe (sphalerite) respectively. Impurities present within vaseline are denoted as ◇.

Estimates of the particle size based on width measurements of the single reflection observed at 42.0° can be made but are not included in this paper because they do not produce accurate values for particles in which distortions and defects occur.

The reaction temperatures and solvents were varied for a series of experiments in order to correlate the reaction conditions with the sizes of the CdSe particles formed and the results are summarized in Table 1.

A change in reaction temperature (see Table 1, Cd1–Cd3) has a large effect on the average particle size as found for analogous runs for CdS and ZnS.[42] PXRD patterns obtained from these samples where the temperature has been varied from −78 to 60 °C, Fig. 3(a)–(c), show significant *hkl* dependent sharpening of lines at higher temperature, *i.e.* an increase in particle size. PXRD studies indicate that the particles exhibit lattice and turbostratic distortions[49,50] (see later) and therefore calculations of the coherence length of the crystallite using a modification of Scherrer's formula[18] give very poor estimations of crystallite size. For a more reliable indication of crystallite diameter, measurements are therefore calculated from TEMs. The type of solvent chosen for the reaction also has a profound effect on the crystallite growth. When light petroleum (bp 40–60 °C) is used (see Table 1, Cd4), the PXRD pattern, Fig. 3(d), is sharper corresponding to an increase in particle diameter.

The PXRD patterns of ZnSe/polymer composites and the JCPDS pattern of hexagonal ZnSe are shown in Fig. 4(a)–(c) where Zn1 [Fig. 4(a)] and Zn2 [Fig. 4(b)] are runs prepared in toluene at −78 °C and r.t. respectively. Again, an increase in reaction temperature corresponds with a sharpening of the *hkl* lines indicating an increase in particle size. The *h*0*l* reflection (103) at 49.5° is clearly observed for Zn1 and is more intense than other high-angle *hkl*. At higher temperature, sample Zn2, all *h*0*l* intensities are suppressed.

The TEM of run Cd2, Fig. 5, shows an even distribution of particles within the polymer matrix. A size distribution graph of a TEM obtained by measuring individual particles on a TEM image of sample Cd2 (run at r.t.) is illustrated in Fig. 6. TEM studies of samples prepared from runs in toluene and electron diffraction of all CdSe samples prepared for TEM confirms the crystallite to have lattice spacings indicative of the Cadmoselite (hexagonal) phase. After two days in an atmosphere of air and after *ca.* 1 week under nitrogen, the colour of the material obtained from sample Cd1 slowly darkened from a yellow to a light brown colour. However, the PXRD patterns taken of the same sample immediately after preparation and then a week later were identical and gave no

Table 1 Dependence of CdSe particle size on various synthesis conditions

run no.	Cd/Py ratio	solvent	*T*/°C	polymer conc. (%)	band gap/eV	av. TEM particle size (range)/nm
bulk CdSe					1.74[a]	
Cd1.	0.5	toluene	−78	3.0	2.72[a]	2.3 (1–4.5)
Cd2.	0.5	toluene	R.T.	3.0	2.17[a]	2.9 (1.0–5)
Cd3.	0.5	toluene	60	3.0	2.15[a]	3.6 (1.5–6)
Cd4.	0.5	light petroleum	25	3.0	2.06[b]	3.1 (1.5–5.5)

Band gap calculated from band edge observed by photoacoustic[a] or absorbance[b] spectroscopy.

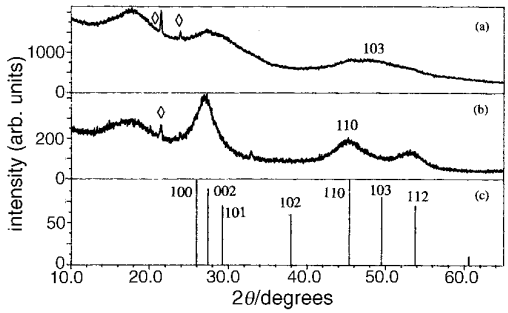

Fig. 4 PXRD patterns of ZnSe prepared in toluene in the presence of 2pySiPB at (a) −78 °C, run Zn1; (b) 25 °C, run Zn2. Pattern (c) corresponds to the JCPDS pattern for hexagonal ZnSe. Impurities present within vaseline are denoted as ◇.

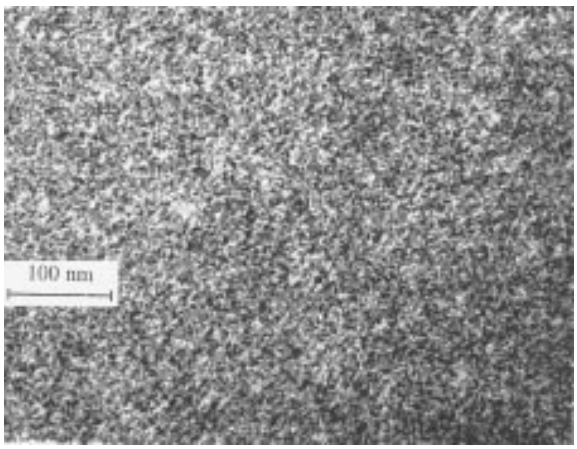

Fig. 5 Low resolution TEM of CdSe particles prepared in run Cd2

sharpening of *hkl* intensities which would be expected if the particle size increased forcing a change in colour (absorbance). This phenomenon is also observed for ZnSe samples and possible explanations will be discussed later.

The band gap of commercial cadmoselite CdSe, as measured from photoacoustic spectroscopy is 1.74 eV (lit. value, 1.70 eV[46]) and differs markedly from those of the CdSe/polymer composites. Photoacoustic spectra [Fig. 7(a)–(c)] obtained from samples Cd1 (−78 °C), Cd2 (r.t.) and Cd3 (60 °C) respectively, show a gradual red shift in the band edge indicating an increase in particle size and a decrease in band gap from 2.72 to 2.15 eV. The UV–VIS absorbance spectrum of the sample prepared in light petroleum [Cd4, Fig. 7(d)] gives a calculated band gap value of 2.06 eV and clearly shows a band edge slope indicative of a large size distribution of particles and exciton relaxation caused by lattice vibrations. In fact, the slopes of the band edges obtained from all samples are shallower than *e.g.* cadmium sulfide samples[42] and could be interpreted as a collective result of (i) lattice vibrations (phonons); (ii) the faster rate at which cadmium selenide particles are formed compared to the sulfides, thus giving a larger and wider particle size distribution due to slower termination of CdSe particle growth (see later); (iii) absorbance transitions to lower energy bands or trapped 'surface' states between the valence and conduction bands which are the result of disrupted crystallite/polymer Cd–N interactions present at the grain boundary formed after particle growth; or (iv) traps between the valence and conduction band which pertain to point defects within the bulk of the nanocrystallite.

The band gap for commercial ZnSe as calculated from the photoacoustic measurement is 2.58 eV (lit. value, 2.58 eV[46]). The photoacoustic measurement of the band edge position for the polymer/composite sample Zn2, Fig. 7(e) is 470 nm,

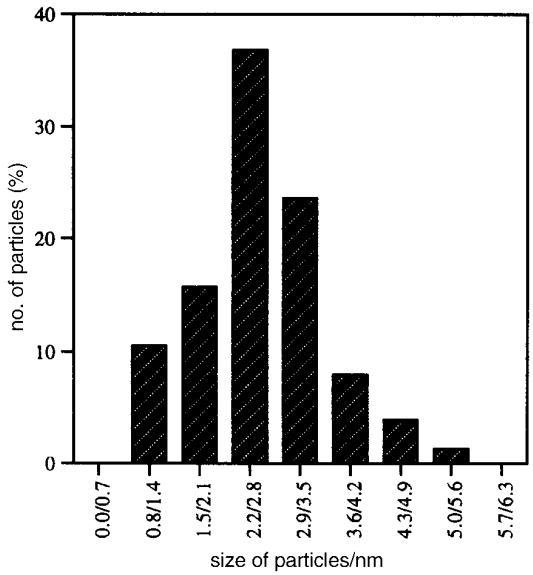

Fig. 6 Size distribution graph of CdSe particles, Cd2, prepared in the presence of 2pySiPB in toluene

(2.63 eV). However, all the band edges observed for samples of this material are very shallow owing to very wide size distributions of particles and lattice vibrations. This observation suggests that the polymer has little control over ZnSe particle growth and termination, reasons for which are discussed shortly.

Many of the composites were investigated for their photoluminescence behaviour. Although blue luminescence was observed for the polymer itself, there was no observable luminescence from the nanoparticles. This is probably because low-lying acceptor orbitals on the pyridine quench the emission.

Discussion

All the PXRD patterns for CdSe samples are consistent with their being of the hexagonal phase. The PXRD pattern of the sample run at high temperature [run Cd3, Fig. 3(c)] suggests that there are turbostratic distortions[49,50] present within the crystallites. A perfect crystal has sharp *hkl* reflections whose structure factors describe the symmetry and contents of the unit cell. If the layer planes are rotated relative to each other the 00*l* reflections remain unchanged; the *hk*0 intensities will change and the peaks will become broadened because the distortions affect the unit cell effectively reducing the crystal size. Most affected will be the *hkl* reflections, similarly reduced in intensity and broadened. These strong characteristics of rotational distortion can be seen in all observed PXRD patterns as the (002) plane is always intense; in most cases the *h*0*l* planes, (101) at 27°, (102) at 35°, (103) at 46°, and the *hkl* plane, (112) at 49.5°, are severely broadened. Distortions involving random shifts of lattice planes along the direction of the specified *hkl* plane of the crystallite give changes in the peak profile exhibiting asymmetry through the peak centre. This effect is observed in the PXRD pattern of run Cd3, Fig. 3(c), where the (110) peak at 42° has a slightly different rate of intensity decay on the high angle side (r.h.s.) of the peak.

In preparations where toluene is the reaction solvent there appear to be fewer stacking faults within these crystallites as compared to previous CdS or ZnS[42] and CdSe samples[18] and this is confirmed by the presence of the (103) reflection in Cd3 [Fig. 3(c)], however, in all cases the (102) reflection is severely broadened and unobserved. While the strong (002) reflection could indicate near perfect registry in this particular lattice

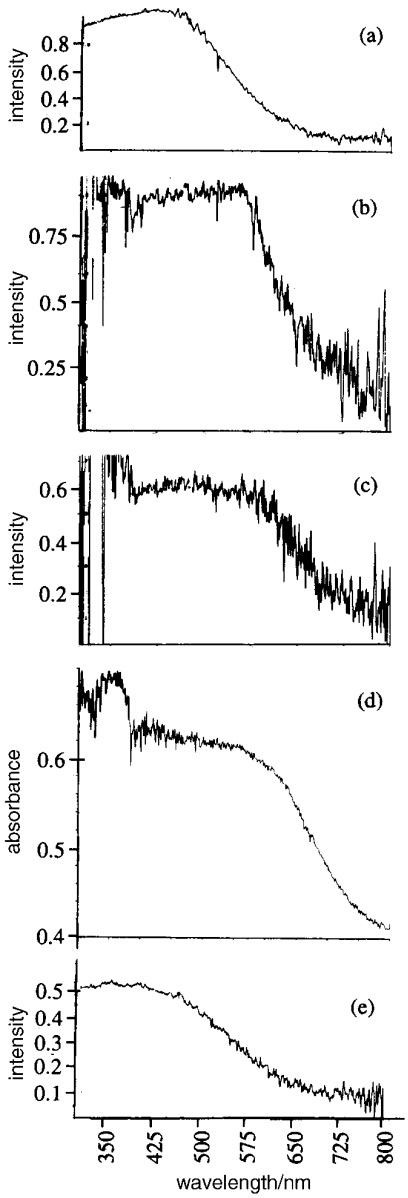

Fig. 7 Photoacoustic spectra of CdSe samples prepared in toluene in the presence of 2pySiPB at (a) −78 °C (run Cd1), (b) r.t. (run Cd2) and (c) 60 °C (run Cd3); absorbance spectrum of a CdSe sample prepared in petrol in 2pySiPB at (d) r.t. (run Cd4); photoacoustic spectrum of a ZnSe sample prepared in toluene in 2pySiPB at (e) r.t. (run Zn1)

plane of the crystallite, another explanation could be a non-uniformity in the crystallite dimensions suggesting preferred orientation along the direction of this plane. Preparations in light petroleum gave a dark brown colouration of the reaction mixture indicating the formation of large sized particles. As similarly found in crystallites formed in analogous reactions for CdS runs, the *h*0*l* reflections are noticeably sharper and the (002) reflection broader than found in other patterns. TEM studies confirm that the particles are agglomerated into clusters with little apparent polymer content but are nevertheless comparable in their size distribution (1.5–4.5 nm) to particles observed in sample Cd3. The cadmium selenide/polymer adduct is insoluble in non-polar light petroleum and thus cannot disperse the growing nanoparticulates and hence allows them to cluster.

The suppression of the (103) plane in the PXRD pattern of the ZnSe sample obtained at room temperature [Zn2, Fig. 4(b)] suggests that there are significant defects within the crystallites, *e.g.* stacking faults.[18] The (002) plane at 27.5° is again the most intense peak in both Zn1 and Zn2 samples. The ZnSe sample obtained at low temperature [Zn1, Fig. 4(a)] shows very broad peaks corresponding to the hexagonal phase of ZnSe at 29.0° (101) and 49.5° (103). The collection of *hkl* intensities around the (002) region observed in Zn2 is narrower than expected which could suggest that the number of stacking faults within the crystallite is comparable with the number of planes in perfect hexagonal registry, hence a substantial percentage of the crystallite co-exists in the form of the cubic phase of ZnSe along with the hexagonal phase. This form of polytypism ensures that the suspected (002) reflection therefore more closely resembles the cubic (111) plane of ZnSe and reinforces the explanation of why the (103) intensity is severely suppressed.

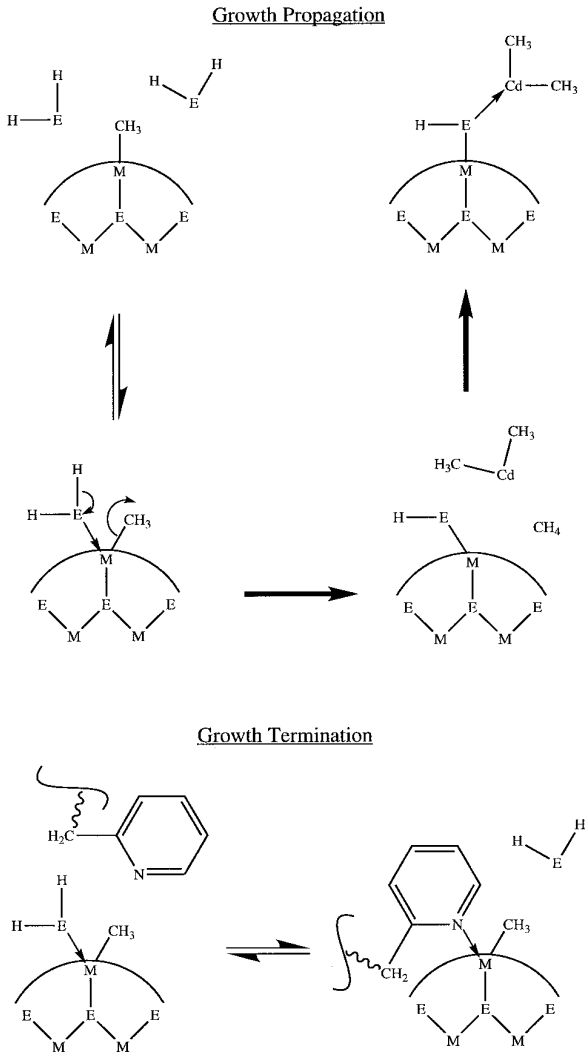

Fig. 8 Propagation and termination of ME (M = Cd, Zn; E = S, Se) particle growth

The region of quantum confinement for CdSe is very narrow and a slight increase or decrease in particle size would clearly lead to a change in colour of the material. However, from our sample observations it has been found that although the colour of the particles (both CdSe and ZnSe) gradually change over a long period of time, the *hkl* dependent line broadening of the PXRD patterns remains unchanged indicating no change in particle dimensions. Therefore, we can consider two possibilities for these observations and firstly, we postulate that on exposure of these samples to moisture a gradual deposition of

red selenium metal on the surface of the particle occurs as oxygen is a harder base than selenium and O_2 thus displaces it forming a colourless, high band gap metal oxide (ZnO, CdO). The second possibility could be the presence of residual hydrogen selenide gas enveloped in the polymer which, on air exposure, decomposes to elemental selenium in a similar manner to selenium alkyls.

On the basis of the average particle size and the size dispersion under a given set of conditions, the effectiveness of the polymer pyridyl group for controlling the growth of nanoparticles appears to decrease in the order ZnS > CdS > CdSe > ZnSe. This is the same order as we have observed in the production of nanoparticles from gas phase reactions of Me_2M and H_2E in the presence of pyridine,[51,52] although in those cases, elemental analysis of the particles obtained gives further information since, for ZnS and CdS there is approximately one mole of pyridine per surface atom, whilst for CdSe much less pyridine is present and for ZnSe there is hardly any pyridine present in the deposits.

We have rationalised these observations in terms of a particle growth model in which surface metal atoms are bound to one methyl group. Since the particle growth is carried out under H_2E-rich conditions, these surface metal atoms bind H_2E. It is the relative rates of elimination of methane (to give surface HE atoms and propagate growth), and displacement of H_2E by pyridine (to terminate growth), that determine the efficiency with which particle growth is controlled by pyridine. For H_2Se, which is much more acidic than H_2S, loss of methane dominates and this is more pronounced for ZnSe because the surface Zn—C bonds are more polar (δ^- on C) than those for Cd. Hence control of growth is poor for the selenides, especially ZnSe. For the less acidic H_2S, the rate of elimination of methane is low, so that the surface bound H_2S adduct has sufficient lifetime for displacement by pyridine, thus terminating growth. The harder nature of Zn than of Cd and of pyridine than of H_2S will ensure that the displacement of H_2S by pyridine will be more favored for ZnS than for CdS. We believe that similar arguments qualitatively explain the growth process and its control for the polypyridine–nanoparticle composites described here. The relevant reaction schemes are shown in Fig. 8.

Conclusions

CdSe semiconductor nanoparticulates in the size range 1–5 nm with a relatively narrow size distribution can be prepared by reacting a polymer adduct solution with H_2Se. When the reaction temperature is controlled and toluene is the reaction solvent, the size of the growing crystallite and hence band edge position can be controlled relatively easily. However, when the solvent is light petroleum, generally wide size distributions of clustered CdSe nanoparticulates are observed, because of the insolubility of the polymer. CdSe nanoparticulates appear to be cadmoselite (hexagonal) in phase and in some cases appear to exhibit partial registry and distortions of the crystallite lattice. Although the quantum confinement regime observed in CdSe is narrow the different colours exhibited by the material in this region as the particles decrease in size are clearly observed indicating that the particle size distribution is relatively small. The particle size of ZnSe semiconductor nanoparticulates is difficult to control mainly because of the strong Brønsted acidity of the hydrogen selenide and its rapid reaction with surface methyl (Zn—Me) groups which carry more negative charge than cadmium methyl groups.

We thank John Mackie at the Bute, St. Andrews, for sample preparation for low resolution TEM. We are also grateful to the Nippon Soda Company for generous gifts of polybutadienes; to Dr Barry Kaye for photography; Professor J. W. Allen and Dr Douglas F. Foster for useful discussions; and the EPSRC for funding (S.H.).

References

1 M. G. Bawendi, M. L. Steigerwald and L. E. Brus, *Annu. Rev. Phys. Chem.*, 1990, **41**, 477.
2 A. Henglein, *Chem. Rev.*, 1989, **89**, 1861.
3 Y. Wang and N. Herron, *J. Phys. Chem.*, 1991, **95**, 525.
4 H. Weller, *Adv. Mater.*, 1993, **5**, 88.
5 H. Weller, *Angew. Chem., Int. Ed. Engl.*, 1993, **32**, 41.
6 J. H. Fendler and F. C. Meldrum, *Adv. Mater.*, 1995, **7**, 607.
7 A. R. Kortan, R. Hull, R. L. Opila, M. G. Bawendi, M. L. Stiegerwald, P. J. Carroll and L. E. Brus, *J. Am. Chem. Soc.*, 1990, **112**, 1327.
8 B. O. Dabbousi, M. G. Bawendi, O. Onitsuka and M. F. Rubner, *Appl. Phys. Lett.*, 1995, **66**, 1316.
9 V. L. Colvin, M. C. Schlamp and A. P. Alivisatos, *Nature* (*London*), 1994, **370**, 354.
10 Y. Yang, J. Huang, S. Liu and J. Shen, *J. Mater. Chem.*, 1997, **7**, 131.
11 Ying Wang and N. Herron, *J. Lumin.*, 1996, **70**, 48.
12 G. Hodes, I. D. J. Howell and L. M. Peter, *J. Electrochem. Soc.*, 1992, **139**, 3136.
13 K. Kalyanasundaram, in *Energy Resources by Photochemistry and Catalysis*, ed. M. Grätzel, Academic Press, London, 1983, p. 217.
14 E. Wolf, *Progress in Optics XXIX*, Elsevier Science Publishers, North Holland, 1991, p. 321.
15 S. H. Risbud, *The Encyclopedia of Advanced Materials*, Cambridge University Press, Cambridge, 1994, p. 2115–2121.
16 E. Corcoran, *Sci. Am.*, 1990, **263**, 74.
17 N. Herron, Y. Wang and H. Eckert, *J. Am. Chem. Soc.*, 1990, **112**, 1322.
18 C. B. Murray, D. J. Norris and M. G. Bawendi, *J. Am. Chem. Soc.*, 1993, **115**, 8706.
19 J. G. Brennan, T. Siegrist, P. J. Carroll, M. Stuczynski, L. E. Brus and M. L. Steigerwald, *J. Am. Chem. Soc.*, 1989, **111**, 4141.
20 T. Trindade and P. O'Brien, *Chem. Mater.*, 1997, **9**, 523.
21 B. Breitscheidel, J. Zieder and U. Schubert, *Chem. Mater.*, 1991, **3**, 559.
22 Y. Wang and N. Herron, *J. Phys. Chem.*, 1987, **91**, 257.
23 X. K. Zhao, L. McCormick and J. H. Fendler, *Chem. Mater.*, 1991, **3**, 922.
24 J. N. Robinson and D. J. Cole-Hamilton, *Chem. Soc. Rev.*, 1991, **20**, 49.
25 Y. Wang, A. Suna, M. Mahler and R. Kasowski, *J. Phys. Chem.*, 1987, **87**, 7315.
26 M. E. Wozniak, A. Sen and A. L. Rheingold, *Chem. Mater.*, 1992, **4**, 753.
27 J. P. Kuczynski, B. H. Milosavljevic and J. K. Thomas, *J. Am. Chem. Soc.*, 1986, **108**, 2513.
28 Y. Wang and W. Mahler, *Opt. Commun.*, 1987, **61**, 233.
29 E. Hilinski, P. Lucas and Y. Wang, *J. Chem. Phys.*, 1988, **89**, 3435.
30 Y. Wang, A. Suna, J. McHugh, E. Hilinski, P. Lucas and R. D. Johnson, *J. Chem. Phys.*, 1990, **92**, 6927.
31 S. Yanagida, T. Enokida, A. Shihdo, T. Shiragami, T. Ogata, T. Fukumi, T. Sakaguchi, M. Mori and T. Sakata, *Chem. Lett.*, 1990, 1773.
32 V. Sankaran, J. Yue, R. E. Cohen, R. R. Schrock and R. J. Silbey, *Chem. Mater.*, 1995, **7**, 1185.
33 (*a*) M. Moffitt and A. Eisenberg, *Chem. Mater.*, 1995, **7**, 1178; (*b*) M. Moffitt, L. McMahon, V. Pessel and A. Eisenberg, *Chem. Mater.*, 1995, **7**, 1185.
34 Y. Yuan, J. H. Fendler and I. Cabasso, *Chem. Mater.*, 1992, **4**, 312.
35 A. Chevreau, B. Phillips, B. G. Higgins and S. Risbud, *J. Mater. Chem.*, 1996, **6**, 1643.
36 L. Spanhel, M. Haase, H. Weller and A. Henglein, *J. Am. Chem. Soc.*, 1987, 109, 5649.
37 A. Iraqi and D. J. Cole-Hamilton, *J. Mater. Chem.*, 1992, **2**, 183 and references therein.
38 P. Narayanan, B. Kaye and D. J. Cole-Hamilton, *J. Mater. Chem.*, 1993, **3**, 19.
39 A. Iraqi, S. Seth, C. A. Vincent, D. J. Cole-Hamilton, M. D. Watkinson, I. M. Graham and D. Jeffrey, *J. Mater. Chem.*, 1992, **2**, 1057.
40 X. Li, C. M. Lindall, D. F. Foster and D. J. Cole-Hamilton, *J. Mater. Chem.*, 1994, **4**, 657.
41 X. Li, J. R. Fryer and D. J. Cole-Hamilton, *J. Chem. Soc., Chem. Commun.*, 1994, 1715.
42 S. W. Haggata, X. Li, J. R. Fryer and D. J. Cole-Hamilton, *J. Mater. Chem.*, 1996, **6**, 1771.

43 X. Li, D. F. Foster and D. J. Cole-Hamilton, *Polym. Adv. Technol*., 1994, **5**, 541.
44 D. J. Cole-Hamilton, *Chem. Br*., 1990, **26**, 852.
45 D. F. Foster and D. J. Cole-Hamilton, *Inorg. Synth*., 1997, **31**, 29.
46 *CRC Handbook of Chemistry and Physics*, ed. D. R. Lide, CRC Press Inc., Boston, MA, 1992, vol. **12**, p. 75.
47 J. I. Pankove, *Optical Processes in Semiconductors*, Dover Publications, New York, 1975, p.43.
48 F. Urbach, *Phys. Rev*., 1953, **92**, 1324.
49 Y. G. Andreev and T. Lundström, *J. Appl. Crystallogr*., 1995, **28**, 534.
50 Y. G. Andreev and T. Lundström, *J. Appl. Crystallogr*., 1994, **27**, 767.
51 N. L. Pickett, D. F. Foster, J. R. Fryer and D. J. Cole-Hamilton, *J. Mater. Chem*., 1996, **6**, 507.
52 N. L. Pickett, D. F. Foster, F. Riddell, J. R. Fryer and D. J. Cole-Hamilton, *J. Mater. Chem*., 1997, **7**, 1855.

Paper 7/01943B; *Received* 19*th March*, 1997